AFRL-OSR-VA-TR-2013-0689

Mechanistic Studies of Metal-Oxo Cubane Catalysts for Lightweight Solar Fuels Storage

Daniel G Nocera

Massachusetts Institute of Technology

March 2013
Final Report

AIR FORCE RESEARCH LABORATORY
AF OFFICE OF SCIENTIFIC RESEARCH (AFOSR)
ARLINGTON, VIRGINIA 22203
AIR FORCE MATERIEL COMMAND

REPORT DOCUMENTATION PAGE

Form Approved
OMB No. 0704-0188

PLEASE DO NOT RETURN YOUR FORM TO THE ABOVE ORGANIZATION.

1. REPORT DATE *(DD-MM-YYYY)*	2. REPORT TYPE	3. DATES COVERED *(From - To)*
22-01-2013	Final	30 Sept 2009 - 31 Dec 2012

4. TITLE AND SUBTITLE

Mechanistic Studies of Metal-Oxo Cubane Catalysts for Lightweight Solar Fuels Storage

5a. CONTRACT NUMBER

5b. GRANT NUMBER
FA9550-09-1-0689

5c. PROGRAM ELEMENT NUMBER

6. AUTHOR(S)

Daniel G Nocera

5d. PROJECT NUMBER

5e. TASK NUMBER

5f. WORK UNIT NUMBER

7. PERFORMING ORGANIZATION NAME(S) AND ADDRESS(ES)

Massachusetts Institute of Technology
77 Massachusetts Avenue
Cambridge MA 02139-4301

8. PERFORMING ORGANIZATION REPORT NUMBER

9. SPONSORING/MONITORING AGENCY NAME(S) AND ADDRESS(ES)

Air Force Office of Scientific Research
875 North Randolph Street, RM 3112
Arlington VA 22203

10. SPONSOR/MONITOR'S ACRONYM(S)

11. SPONSOR/MONITOR'S REPORT NUMBER(S)
AFRL-OSR-VA-TR-2013-0125

12. DISTRIBUTION/AVAILABILITY STATEMENT

Distribution A: Approved for public release

13. SUPPLEMENTARY NOTES

14. ABSTRACT

The use of solar energy for mobile field operations, high altitude long endurance airships, light airship vehicles and its deployment on large scales all require its storage. Most current methods of solar storage are characterized by low energy densities; these methods therefore present formidable challenges for the implementation of solar energy in the field, on airship vehicles and on the large scale since significant weight accompanies energy storage. Conversely, fuels have energy densities that are 100 to 1000 greater than most conventional storage media, including batteries. Accordingly, fuels provide an attractive option for lightweight, mobile and large scale energy storage. An especially enticing fuel forming reaction is water splitting since hydrogen is the highest energy density chemical fuel. The use of solar light to split water to produce hydrogen and oxygen is the focus of this proposal. This AFOSR program has sought to discover new water-splitting catalysts that are inexpensive, efficient, highly manufacturable and operate under benign conditions so that discovery from this program may be implemented with simple engineering.

15. SUBJECT TERMS

biomimetic, artificial, photosynthesis, high altitude vehicles, solar, energy, clusters, catalysis, corrosion. self-healing, leaf

16. SECURITY CLASSIFICATION OF:			17. LIMITATION OF ABSTRACT	18. NUMBER OF PAGES	19a. NAME OF RESPONSIBLE PERSON
a. REPORT	b. ABSTRACT	c. THIS PAGE			Richard J. Wilk
U	U	U	U		19b. TELEPHONE NUMBER *(Include area code)* (617) 253-1802

Reset

Standard Form 298 (Rev. 8/98)
Prescribed by ANSI Std. Z39.18

AFOSR Final Performance Report

Title:	Mechanistic Studies of Metal-Oxo Cubane Catalysts for Lightweight Solar Fuels Storage
Grant. Number:	FA9550-09-1-0689
Original Program Manager:	Walter Kozumbo Air Force Office of Scientific Research 875 North Randolph Street 4027 Arlington VA 22203
Current Program Manager:	Dr. Patrick O. Bradshaw Air Force Office of Scientific Research 875 North Randolph Street 4027 Arlington VA 22203 Email: Patrick.Bradshaw@afosr.af.mil
Principal Investigator:	Daniel G. Nocera Department of Chemistry, 6-335 Massachusetts Institute of Technology 77 Massachusetts Ave. Cambridge, MA 02139-4307 U.S.A. Email: dnocera@fas.harvard.edu

Summary of Accomplishments/New Findings

This AFOSR grant has emphasized homogenous molecular models to provide mechanistic insights into the operation of water splitting catalysts. Highlights of the molecular work include:

1. Measurement of their EPR spectra of Co_4O_4 cubanes and comparison these spectra to those of the authentic Co–OEC catalysts, This work has allowed us to ascertain the delocalization of the Co(IV) holes in a cluster species possessing a structure that is akin to the Co–OECs. This work has been pivotal in providing an understanding of the pre-catalytic state, and providing a framework in which to develop a rational mechanism for O–O bond formation by the Co–OEC catalysts.
2. A penetrating study of $Co^{3+}|Co^{4+}$ self-exchange kinetics of Co_4O_4 cubanes and a detailed understanding of their mechanism of proton-coupled electron transfer (PCET). This work has (i) modeled PCET activation features of the Co–OEC catalysts and (ii) provided an understanding of how hole transfer propagates through films of the active Co–OEC catalysts.
3. A fundamental understanding of Co–OEC catalyst activity. This latter insight led directly to the realization of highly active catalysts films. Moreover, knowledge of the mechanism was needed to construct the artificial leaf described in (7).
4. The examination of $Co^{2+}|Co^{3+}$ self-exchange in a faithful structural molecular analog of the 7 atom cobalt cluster, thus allowing us, together with (2), to define the electron transfer kinetics of the complete Co(II)-Co(III)-Co(IV) cycle of the Co–OEC catalysts using molecular analogs of the catalyst .

The other major advance of this AFOSR program was the integration of the Co-Ni|Pi-Bi catalysts with Si and the creation of the artificial leaf. Highlights of AFOSR work during the previous funding cycle include:

5. Methods for electro- and photo- depositing the Co–OEC catalyst onto crystalline-silicon (c-Si) and amorphous-silicon (a-Si).
6. Characterization of OER reactivity driven by single junction c-Si.
7. Characterization of OER reactivity driven by a triple junction a-Si solar cell and the construction of an artificial leaf composed of earth abundant materials. The leaf works under simple conditions (out of any container of any type of water source under ambient conditions).
8. The development of a new OER Ni–OEC catalyst that has Tafel slope that is optimized to the peak performance of Si PV materials near the thermodynamic potential of water splitting.

1. Objectives

Molecular catalysts were developed to provide insights into the function of heterogeneous, thin film, water-splitting catalyst, Co–OEC and Ni–OEC. The molecular systems provide a means of interrogating intimate details, often inaccessible in heterogeneous materials, of these kinetically demanding chemical transformations. These studies are necessary to understand the processes of OER at its most fundamental level and to provide a framework for the rational design of more active OEC systems. On the foundation of this mechanistic understanding, catalyst integration with silicon was sought to create the artificial leaf.

2. Findings

2.1. A Structural Molecular Model of Co–OEC Catalysts

The CoP_i catalyst is a functional and related structural model of PSII–OEC. Shown in Figure 1 are the structures of the PSII–OEC[1] and the core structure of CoP_i as deduced from X-ray absorption spectroscopy.[2,3] Both PSII–OEC and CoP_i have a partial cubane structure. In OEC, the cube is completed with a Ca^{2+} ion; though the alkali metal ions for CoP_i have not been located, they likely reside on the three-fold oxygen triangle to complete the cube structure, as is the case for cobaltates.[4] As highlighted in Figure 1, CoP_i is the corner-sharing head-to-tail dimer of PSII–OEC. The metal-metal (d = 2.8 Å) and metal-oxo (d = 1.9 Å) distances in CoP_i and PSII–OEC are similar. A view of the dicubane structure rotated by 45° is also shown in Figure 1. In this view, it is easier to see that CoP_i consists of edge-sharing CoO_6 octahedron, which is the basic building block of alkali metal cobaltates.[5] The edge Co atoms of the cluster are terminated by the phosphate ions, which have been shown to be exchangeable.

The 7-atom molecular cluster may be stabilized by 2-methoxy[(methylimino)methyl]-phenol (HL), **1**.[6] This cluster, which is shown in Figure 2, has the precise Co-oxo core of

---

1 "Crystal structure of the oxygen-evolving complex of photosystem II." Barber, J. *Inorg. Chem.* **2008**, *47*, 1700.

2 "Cobalt-oxo core of a water-oxidizing catalyst film." Risch, M.; Khare, V.; Zaharieva, I.; Gerencser, L.; Chernev, P.; Dau, H. *J. Am. Chem. Soc.* **2009**, *131*, 6936.

3 "Structure and valency of a cobalt phosphate water oxidation catalyst determined by in situ x-ray absorption spectroscopy." Kanan, M. W.; Yano, J.; Surendranath, Y.; Dincă, M.; Yachandra, V. K.; Nocera, D. G. *J. Am. Chem. Soc.* **2010**, *132*, 13692.

4 "Single-crystal growth, crystal and electronic structure of $NaCoO_2$." Takahashi, Y.; Gotoh, Y.; Akimoto, J. *J. Sol. State Chem.* **2003**, *172*, 22.

5 "Charge transfer, hybridization and local inhomogeneity effects in $Na_xCoO_2 \bullet yH_2O$: An x-ray absorption spectroscopy study." Poltavets, V. V.; Croft, M.; Greenblatt, M. *Phys. Rev. B* **2006**, *74*, 125103.

6 "Traditional and microwave-assisted solvothermal synthesis and surface modification of Co_7 brucite disk clusters and their magnetic properties." Zhou, Y.-L.; Zeng, M.-H.; Wei, L.-Q.; Li B.-W.; Kurmoo M. *Chem. Mater.* **2010**, *22*, 4295.

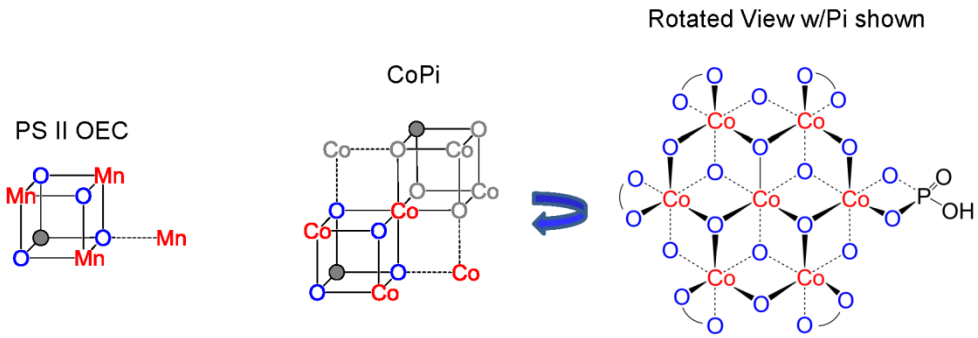

Figure 1. (Left) Schematic of cubane structure of PSII–OEC. (Middle) Structure of the CoP_i as determined from EXAFS (P_i not shown). Co–OEC is the head-to-tail dimer of the cubane of PSII–OEC. (Right) CoP_i structure rotated by 45° to more clearly show edge sharing octahedra.

CoP_i.[3] All of the cobalt atoms in this molecule are divalent. We have developed a high yield synthesis of **1** and have found that the central Co^{2+} atom can be oxidized to Co^{3+}. This one-electron oxidized core, **2**, can be isolated and also structurally characterized. Our high yield synthesis of the cluster in the Co^{2+} and Co^{3+} states has allowed us to undertake detailed studies of the $Co^{2+}|Co^{3+}$ self-exchange kinetics, which is a critical factor in the formation of CoP_i films because self-assembly occurs upon the oxidation of Co^{2+} to Co^{3+} in the presence of B_i, P_i or MeP_i.

We have found that the inner bridging hydroxide ligands provide a pathway for redox-leveling by PCET. Remarkably, both clusters **1** and **2** have readily interpretable and distinctive NMR spectra thus allowing us to examine this PCET process. Using the deuterium-labeled ligand (HL*), self-exchange electron transfer between **1*** and **2** has been examined by time-resolved, variable-temperature NMR spectroscopy. The McKay equation, which relates the rate of isotope exchange to the rate of electron transfer,[7]

$$-\ln\left(1-\frac{[Red]_t}{[Red]_\infty}\right)=\frac{R_{ex}(C_{Red}+C_{Ox})}{C_{Ox}\cdot C_{Red}}t \qquad (1)$$

has shown us that the $Co^{2+}|Co^{3+}$ electron transfer for the cobalt residing in the central oxidic ligand field of the cluster is many orders of magnitude slower than that of hexa-aqua $Co_{aq}^{2+/3+}$ self-exchange.[8] We have concluded that $Co^{2+}|Co^{3+}$ self-exchange is dependent on an inner-sphere mechanism. Since the cluster geometry precludes the inner-sphere mechanism in the case of **1** and **2**, the slow electron transfer between these molecules suggests that the fast electron transfer in the $Co_{aq}^{2+/3+}$ couple is actually mediated by a water-bridging inner-sphere mechanism. Our studies resolve a three decade controversy

---

7 "Kinetics of exchange reactions." McKay, H. A. C. *Nature* **1938**, *142*, 997.

8 "Electron-transfer reactions between aqueous cobaltous and cobaltic ions." Habib, H. S.; Hunt, J. P. *J. Am. Chem. Soc.* **1966**, *88*, 1668.

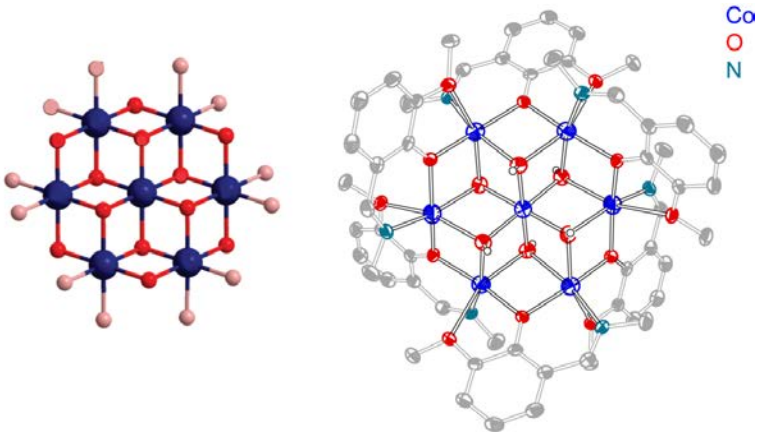

Figure 2. (Left) CoP_i structure emphasizing cluster core. (Right) A molecular analog of CoP_i. The cluster core is emphasized and the 2-methoxy[(methylimino)methyl]phenol ligands of the core are gray-scaled. The molecular analog has been synthesized, isolated and structurally characterized for the central metal of the cluster in both the Co^{2+} and Co^{3+} oxidation states, thus allowing for the examination of the $Co^{2+}|Co^{3+}$ electron transfer kinetics.

for $Co^{2+}|Co^{3+}$ self-exchange.[9,10] Of pertinence to this program, the work provides insight into the participation of Co(II) in the formation and operation of the CoP_i catalyst.

2.2. EPR Studies of Molecular Co-oxo Cubanes as Related to CoP_i

CoP_i catalyst films exhibit EPR signals corresponding to populations of both Co(II) and Co(IV). Figure 3 shows the EPR spectrum of CoP_i under deposition conditions and as compared to Co(II) containing species (top panel, left), CoP_i under an applied voltage at which catalysis occurs (middle panel, left) and a Co_4O_4 cubane containing cobalt in the +4 oxidation state (bottom panel, left). The presence of Co(IV) is clearly established at potentials that OER catalysis occurs. As the deposition voltage is increased into the region where water oxidation prevails (right panel), the population of Co(IV) rises and the population of Co(II) decreases.

Recent studies have taken the EPR of the Co_4O_4 cubane of Figure 3 one step further. The cobalt tetramer has a total electron spin S = ½ and formal cobalt oxidation states III, III, III and IV. The Davies ENDOR spectrum in Figure 4 is well-modeled using a single class of hyperfine-coupled ^{59}Co nuclei with a modestly strong interaction (principal elements of the hyperfine tensor are equal to [–13 –23 80] MHz). Mims ^{1}H ENDOR spectra of the cubane

---

[9] "Kinetics of oxidation of metal complexes by manganese(III) aquo ions in acidic perchlorate media: The $Mn(H_2O)_6^{2+}$–$Mn(H_2O)_6^{3+}$ electron-exchange rate constant." Macartney D. H.; Sutin, N. *Inorg. Chem.* **1985**, *24*, 3403.

[10] "Examination of the intrinsic barrier to electron transfer in hexaaquocobalt(III): Evidence for very slow outer-sphere self-exchange resulting from contributions of Franck–Condon and electronic terms." Endicott, J. F.; Durham, B.; Kumar, K. *Inorg. Chem.* **1982**, *21*, 2437.

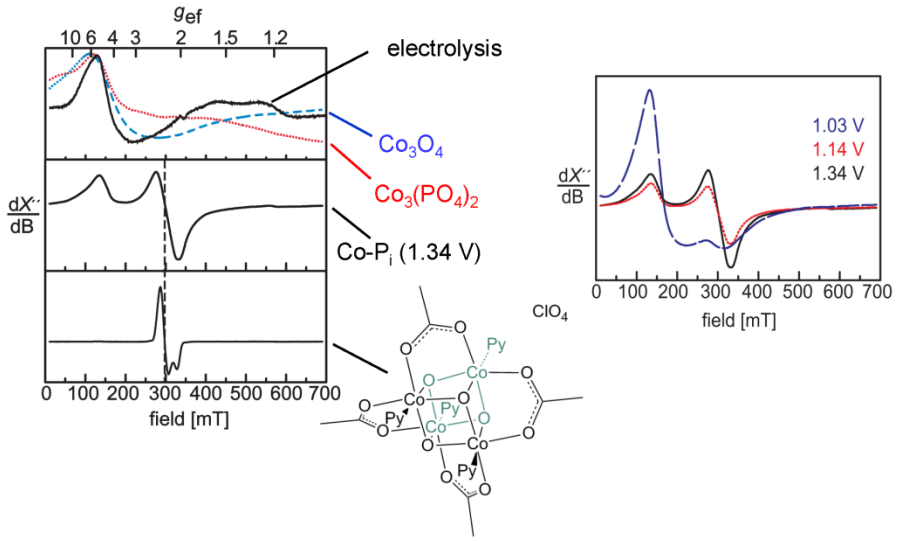

Figure 3. CW X-band EPR spectra of (left, top) frozen electrolysis solution (—), $Co_3(PO_4)_2$ (▪▪▪▪), Co_3O_4 (— —), (left middle) CoP_i catalyst films deposited at 1.34 V, and (left bottom) the Co-oxo cubane $[Co_4O_4(C_5H_5N)_4\text{-}(CH_3CO_2)_4](ClO_4)$, which exhibits an EPR signal for Co(IV) at g = 2.27. Vertical dotted line indicates g = 2.27 resonance as compared to the predominant resonance of frozen CoP_i at potentials at which OER catalysis takes place. T = 5.7 K; Microwave power = 1.02 mW. (right) Potential dependence of EPR spectrum from 1.03 V, at which catalysis does not occur to 1.34 V, at which catalysis occurs.

with selectively deuterated pyridine ligands confirm that the amount of unpaired spin on the cobalt-bonding partner is significantly reduced from unity. Multifrequency ^{14}N ESEEM spectra (acquired at 9.5 and 34.0 GHz) indicate that multiple equivalent ^{14}N nuclei are coupled to the electron spin. Cumulatively, these EPR spectroscopic findings indicate that the unpaired spin is delocalized almost equally across the cobalt core atoms, a finding corroborated by results from DFT calculations. These results suggest that the charge on the CoP_i catalyst is also highly delocalized.

2.3. PCET Studies of Cobalt-Oxo Cubane

EPR studies establish Co(IV) as the oxidation state from which the OER occurs. We thus wished to define (i) the PCET kinetics of Co^{4+} in a cubane environment and (ii) the $Co^{3+}|Co^{4+}$ self-exchange kinetics, which define how the catalytically active "holes" propagate from the electrode through an active catalyst film. We have done so by defining the kinetics for the reaction cycle shown in Figure 5 for the molecular Co_4O_4 cubane compound, $[Co_4O_4(O_2CMe)_2\text{-}(bpy)_4](ClO_4)_2$ (**3**).[11]

Compound **3** is a structural relative of CoP_i, as both are able to stabilize Co(III)|Co(IV) mixed valency within a cubane-like geometry bridged by μ_3-O/OH moieties. The pH

[11] "Dimerization of the $[Co_2^{III}(OH)_2]$ core to the first example of a $[Co_4^{III}O_4]$ cubane: Potential insights into photosynthetic water oxidation." Dimitrou, K.; Folting, W. E.; Streib; Christou, G. *J. Am. Chem. Soc.* **1993**, *115*, 6432.

dependence of the Co(III) to Co(IV) redox potential was measured, revealing a pK_a of ~3.1 for the protonated cube (**3-H$^+$**). For *bidirectional* PCET (ET and PT *not* in the same direction) a near-Nernstian slope at pH < 3 (Figure 6) is consistent with a one-electron, one-proton transfer from **3-H$^+$** to the oxidized molecule (**4**). The absence of a kinetic isotope effect (KIE) coupled with an inverse dependence on H^+ activity is ascribed to a PCET mechanism that is stepwise with an equilibrium proton transfer followed by a rate-limiting electron transfer (PTET).[12] The kinetics for this bidirectional PCET were measured by chemical means using the one-electron transfer reagent $Ru(bpy)_3^{2+}$ and by following the reaction using stopped-flow spectroscopy in H_2O and D_2O under pseudo-first order conditions. From this data, a second-order rate constant of ~1.3×10^6 M^{-1} s^{-1} was derived. The lack of a KIE is again consistent with a stepwise process.

The self-exchange (SE) PCET mechanism is a *unidirectional* PCET between **3-H$^+$** and **4,**

3-H$^+$ + 4* → 4 + 3*-H$^+$ (2)

Using NMR line-broadening techniques, the kinetics for the unidirectional PCET were shown to stand in contrast to those of the above bidirectional case. The second-order rate constant for reaction (2) was 1.3×10^4 M^{-1} s^{-1} at pH 1, two orders of magnitude lower than in the stepwise mechanism. At pH 4, where **3** is deprotonated, the rate constant increases by a factor of 10, to 3×10^5 M^{-1} s^{-1}, consistent with a simple electron transfer step. A KIE of 4.3 is suggestive of a change in mechanism from bidirectional PTET to unidirectional concerted proton-electron transfer (CPET). We have shown

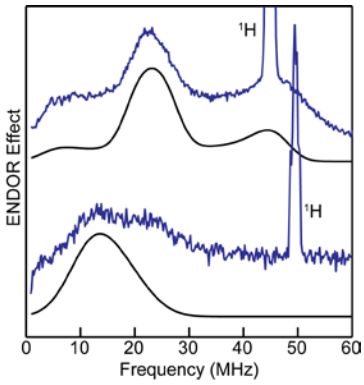

Figure 4. ENDOR of oxidized Co_4O_4 cubane (blue) taken at the perpendicular (top) and parallel (bottom) turning points of the EPR spectrum. Simulation of spectrum (black).

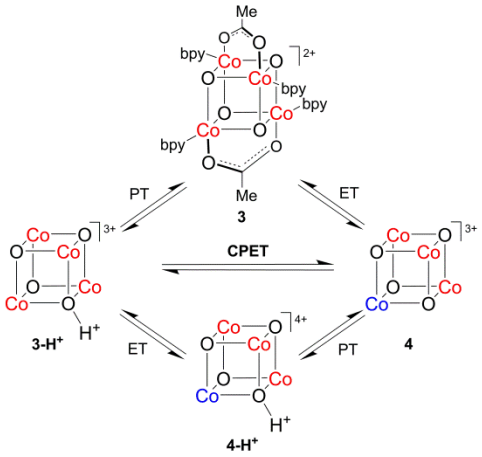

Figure 5. Square scheme for PCET mechanism of Co^{3+} and Co^{4+} in a Co-oxo cubane environment.

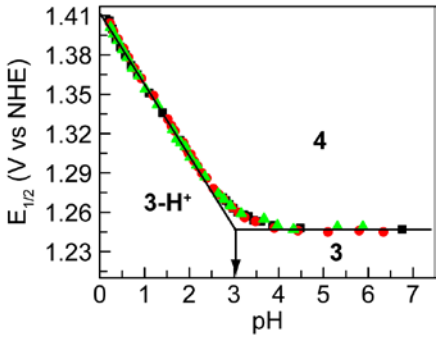

Figure 6. Pourbaix diagram of cubane **3**. Labels on the plot indicate zones of thermodynamic stability for **3**, **3-H$^+$**, and **4**.

[12] "Concerted proton–electron transfers: Electrochemical and related approaches." Costentin, C.; Robert, M.; Savéant, J.-M. *Acc. Chem. Res.* **2010**, *43*, 1019.

that CPET results in order to avoid the high energy barrier of >0.16 V posed by intermediate **4-H$^+$**. This result provides a framework for understanding the magnitude of the energetic penalties that are responsible for PCET mechanism changes in processes important for the efficient functioning of CoP_i. Moreover, this establishes the mechanism for hole propagation through films of the catalyst.

2.4. Mechanistic Studies of CoPi Based on Molecular Systems and Highly Active Catalyst Films

The molecular studies establish that OER catalysis occurs among a Co(II)-Co(III)-Co(IV) cycle and that the pre-catalytic state is Co(IV). With this understanding, detailed electrokinetic studies of the mechanism of CoP_i were undertaken.

The measured current density for electrochemical water oxidation is directly proportional to the velocity of O_2 evolution. Therefore, the determination of the steady-state activation-controlled current density, i, as a function of various parameters, such as potential, pH and electrolyte concentration, enables construction of an electrochemical rate law, from which a mechanistic hypothesis may be developed. A key measurement in electrocatalysis is the evaluation of the logarithm of i as a function of the applied potential, E, or overpotential, η. The slope of the resulting Tafel plot gives insight into the nature of the electrochemical steps preceding and involved in the turnover-limiting step (TLS) of O_2 evolution. We found that the Tafel plots (Figure 7) of CoP_i films display a slope of 60 mV/decade irrespective of film thickness, indicating this indicates that the kinetic profile of catalyst films is not influenced by barriers to charge and/or mass transport through catalyst films. Furthermore, the independence of the Tafel slope on rotation rate, when films were electrodeposited onto a rotating disk electrode, demonstrated that this 60 mV/decade Tafel slope is representative of the kinetics of active sites under activation-control—the absence of mass transport limitations through solution. A 60 mV/decade Tafel slope indicates that there exists a one-electron pre-equilibrium, prior to a chemical turnover limiting step (i.e. the TLS does not involve electron transfer away from the active site). In addition, the steady-state electrode potential decreases by 60 mV per pH unit (Figure 7) indicating a one-electron, one-proton PCET conversion prior to the TLS. A zeroth reaction order in phosphate concentration [P_i] indicated the absence of a

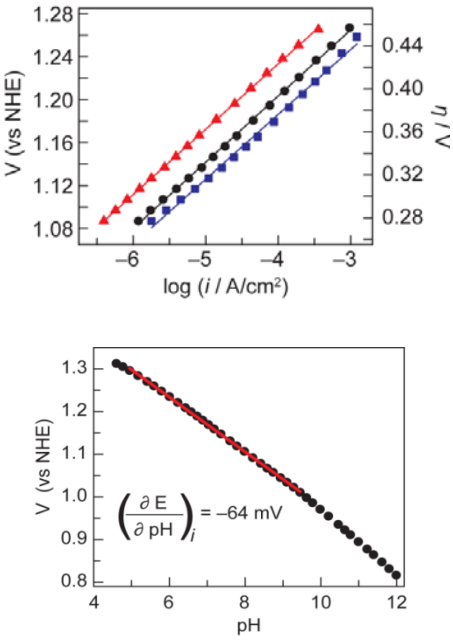

Figure 7. (top) Tafel plots V = (V_{appl} – iR), η = (V – E^0) of CoP_i films deposited on FTO by passage of 6 (▲), 24 (●), and 60 (■) mC cm^{-2}. (bottom) pH dependence on potential at a constant current density of 30 μA cm^{-2}.

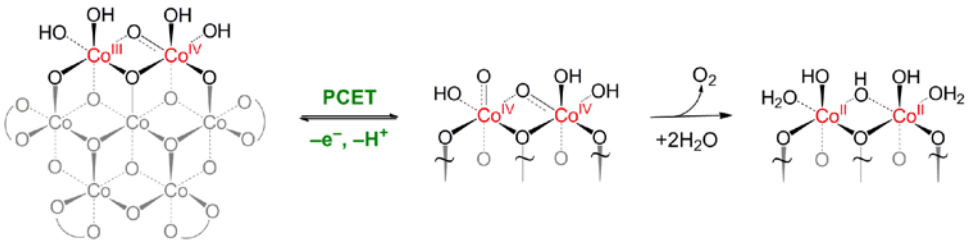

Figure 8. The OER mechanism of CoP_i as determined from electrokinetic, in situ spectroscopic and molecular self-exchange kinetics studies. Curved lines denote phosphate, or OH_x terminal or bridging ligands.

turnover-limiting PT and completed the electrochemical rate law for water oxidation on CoP_i:

$$j = k_0(a_{H^+})^{-1} \exp\left[\frac{EF}{RT}\right] \tag{3}$$

With the results of the molecular studies, we determined that PCET pre-equilibrium was a Co^{3+}–OH to Co^{4+}–O transformation followed by a TLS of O–O bond formation. The overall mechanism of OER catalysis involves a Co(II) to Co(III) to a Co(IV) oxidation cycle. The catalytically active state is delivered by a PCET pre-equilibrium shown in Figure 8. Key assumptions regarding the fundamental exchange rate of terminal and bridging oxygen atoms remain to be addressed in future studies with appropriate molecular models.

Unlike crystalline extended solids, catalysis is not confined to the exterior surface of Co–OECs. In Co–OEC, which is composed of molecular units arranged in a porous network, OER catalysis occurs throughout the film. With the mechanism and self-exchange kinetics in hand, we have been able to construct highly active films of the Co–OECs (CoP_i and CoB_i).

Electrodeposition of Co–OECs on three-dimensional open cell Ni foam substrates delivers highly active O_2 evolving anodes. These anodes exhibit sustained water oxidation at 100 mA/cm^2 at 442 and 363 mV overpotential for films operated in P_i and B_i electrolytes respectively. We have also demonstrated that Co–OEC retains water oxidation activity when operated at neutral pH in natural water sources derived from the Charles River (Cambridge, MA) and Atlantic Ocean (Woods Hole, MA). This is in stark contrast to commercial OER catalysts, which exhibit a rapid loss in activity when operated in unpurified natural waters.

2.5. The Artificial Leaf

Interfacing fuel-forming catalysts with light-harvesting semiconductors affords a pathway to direct solar-to-fuels conversion that captures the basic elements of a leaf. In nature, photosynthetic organisms like plants convert the energy of sunlight into chemical energy

by splitting water, producing molecular oxygen and hydrogen equivalents.[13] After a photon is absorbed by chlorophyll and other pigments, its energy is transferred to the reaction centre of PSII, where a single electron/hole charge separation occurs. The electron is transferred to the adjacent Photosystem I (PSI), where it participates in the reduction reaction of NADP into NADPH. The oxidative power of the photo-produced hole in PSII is transferred to the OEC where water splitting occurs after the accumulation of four hole equivalents.

An 'artificial leaf' can be designed if the one-electron/hole wireless current of a semiconductor can be integrated directly with catalysts to perform the four electron-four proton catalysis of water splitting. With technology transitions in mind, we settled on using Si as a semiconductor because silicon is currently the most widely used material for photovoltaic applications. Also, decades of research have resulted in low losses associated with bulk and interfacial carrier transport.

2.5.1. Catalyst Integration to Si PV

To realize an efficient artificial leaf, it is crucial that photogenerated charge carriers migrate freely from the PV to the catalysts. In other words, an Ohmic contact must be established between the PV element and the catalytic sites, allowing for charge transport with minimum voltage drops.

We have shown that we can use a Si as a substrate for processing of cobalt metal films from which the CoP_i can be grown directly. Under illumination, these CoP_i-coated photoanodes exhibited a 0.35 V reduction in the onset potential for the OER. In addition, we have also prepared a composite photoassisted anode by sputtering a 50 nm film of ITO on the *p*-side of the silicon *pn*-junction followed by annealing (400 °C, N_2, 30 min). The ITO layer serves to protect the Si from oxidation during operation. An optional p^+ layer was incorporated between the *p*-Si and the ITO layer depositing a 1 μm film of silicon-doped (1%) Al on the *p*-side of the junction, followed by rapid thermal annealing in N_2 at 900 °C.[14] The CoP_i catalyst was then electrodeposited on the ITO barrier layer. The performance of these ITO-passivated Si anodes is discussed in the next section.

2.5.2. Single Junction PEC Cell

The single junction npp^+ cell shown in Figure 9 was prepared. A metal front contact (Ti/Pd/Ag, 20/20/100 nm thickness, respectively) was deposited on the *n*-side of the sample to enable PEC measurements and was protected from the solution using a 10 μm

---

[13] "Biological solar energy." Barber, J. *Phil. Trans. Roy. Soc. A* **2007**, *365*, 1007.

[14] "An optimized rapid aluminum back surface field technique for silicon solar cells." Narasimha, S.; Rohatgi, A.; Weeber, A. W. *IEEE T. Electron Dev.* **1999**, *46*, 1363.

layer of photoresist. The CoP_i film was electrodeposited onto the ITO layer using our well-established method (see above).

Figure 10 shows a comparison of the CV curves of *np*Si-ITO-Co–OEC and *npp*$^+$Si-ITO-Co–OEC immersed in a 0.1 M KP_i electrolyte at pH 7. Under these conditions, the thermodynamic potential for water oxidation is 0.82 V relative to the formal normal hydrogen electrode (NHE). When applying the potential through the ITO thin film in the dark (blue traces in Figure 10), the voltammograms indicate that overpotentials in excess of 0.4 V are required to attain current densities on the order of 1 mA/cm^2. This is in agreement with the activity profile for CoP_i on ITO or FTO electrodes. When applying the potential through the metal contacts, such that current must flow through the PV component, the observed dark currents are much lower (black traces in Figure 10).

When illuminating the structure from the *n*-side with 100 mW/cm^2 of AM 1.5 light, the potential onset for water oxidation is decreased significantly for both the *np*Si-ITO-Co–OEC and the *npp*$^+$Si-ITO-Co–OEC samples (green lines in Figure 10). Noting that this single junction cell generates 0.57 V, we see that the onset of the cell under illumination requires 0.52 V less applied potential to induce the OER, indicating that the majority of the photo-voltage generated by the solar cell is utilized to drive the OER. The *npp*$^+$-Si single junction displays improved performance because the space charge region in the p^+ layer is thin enough to act as a tunneling layer. As a result, the p^+-Si/ITO interface behaves as an Ohmic contact for hole transport.

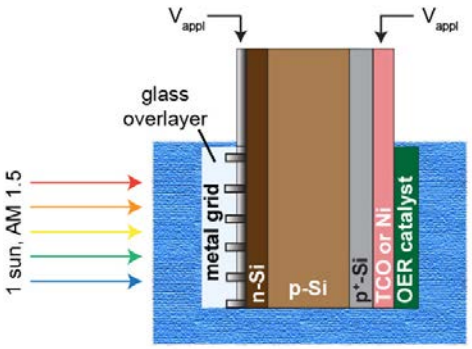

Figure 9. Schematic of a CoP_i functionalized *npp*$^+$-silicon single-junction PEC cell.

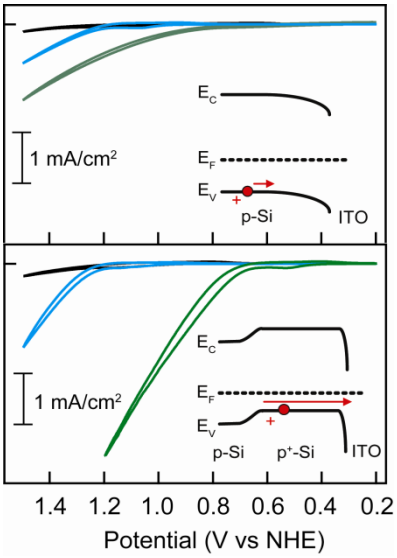

Figure 10. CV curves of Si-ITO-Co–OEC samples (top) without and (bottom) with a p^+-layer. Samples were immersed in a 0.1 M KP_i electrolyte in dark (black line) and illuminated with a Xe lamp (green line, intensity ~100 mW/cm^2). The powder blue curves correspond to the dark CV curve when the potential was applied through the ITO film at the back contact.

Figure 10 highlights that a detailed understanding of the PV-catalyst interfaces is essential for realizing efficient artificial leaves. Current work seeks to optimize the various elements in the leaf, focusing on the Ohmic nature of the contact, chemical stability of the passivating layer and OER and HER catalysts activity.

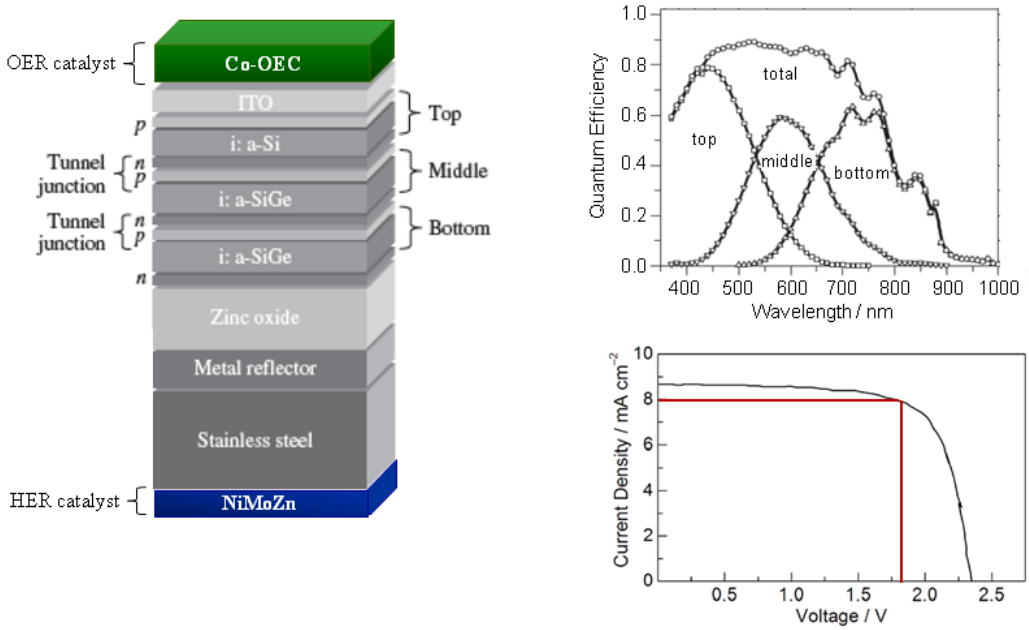

Figure 11. The artificial leaf. The *p*-side of 3jn-a-Si solar cell is coated with an ITO layer and CoP_i. The *n*-side is coated with a new HER catalyst developed in our labs. The overall 3jn-a-Si under AM 1.5 illumination, water splitting is achieved.

2.5.3. Triple Junction PEC Cell: The Artificial Leaf

Stand-alone operation of the cell with no external applied potential from an electrical power source (i.e., unassisted) was performed by interfacing CoP_i with a triple junction amorphous Si (3jn-a-Si) solar cell. The architecture is shown in Figure 11. The CoP_i|3jn-a-Si photoanode drives the OER for O_2 production, and a new NiMoZn cathode drives the HER for H_2 production. The 3jn-a-Si produces 8 mA cm^{-2} of current at 1.8 V. When the wireless CoP_i|3jn-a-Si|NiMoZn wafer is immersed in an open container of electrolyte (1 M potassium borate, pH 9.2) and illuminated with 1 sun (AM 1.5 simulated sunlight), O_2 bubbles evolve from the anode at the front face and bubbles of H_2 evolve from the cathode at the back of the wireless cell. The overall solar-to-fuels efficiency (SFE) can be as high as 4.7% when Ohmic losses are minimized. Noting that the light-to-electricity efficiency of 3jn-a-Si is φ(PV) = 7.7%,

$$\text{SFE}\ (\%) = \varphi(\text{PV}) \bullet \varphi(\text{WS}) \qquad (4)$$

yields an overall efficiency for water splitting of φ(WS) = 60%. This value compares well with cell efficiencies based on 3jn-a-Si PVs in which the a-Si is isolated from the electrolyte (SFE = 6% for φ(PV) = 10%)[15-17] and for higher-efficiency systems using expensive PV

[15] "High-efficiency integrated multijunction photovoltaic/electrolysis systems for hydrogen production." Khaselev, O.; Bansal, A.; Turner, J. A. *Int. J. Hyd. Energy* **2001**, *26*, 127.

materials (SFE = 18% for φ(PV) = 28%).[15,18,19] Based on φ(WS), higher overall cell efficiencies (>10%) may be readily achieved through the use of more efficient PVs.

The integration of earth-abundant water splitting catalysts with photovoltaic silicon cells captures the functional elements of energy capture and storage by a leaf. The ability to drive water splitting directly without the use of wires under a simply engineered configuration opens several new avenues of exploration (*vide infra*).

2.6. A Nickel-Based OEC

In the PV-PEC configuration, the photovoltage generation and current rectification occur at the *np*-junction buried within the silicon solar cell. Thus, it is the intersection of the *i*-V curve of the PV component with the *i*-V curve of the OER catalyst that dictates the (photo)potential and (photo)current utilized for water splitting.[20] This is shown in Figure 12. The red curve is the PV *i*-V curve of the 3jn-a-Si. The blue curve describes the electrochemical load of the PV-PEC. This curve is generated based on known metrics of the OEC (in this case CoP_i) and HER catalyst Tafel behavior, and on estimates for the solution resistance. The SFE is nearly optimal with the electrochemical activity intercepting the PV curve near its maximum power point. However, as the PV curve is moved closer to the thermodynamic potential for water splitting (e.g. when using a PV unit with a lower V_{oc}, see red dashed curve), the SFE drops dramatically when using CoP_i (Tafel slope = 60 mV/decade). However, the SFE is recovered if the Tafel slope of the OEC decreases from 60 mV to 30 mV per decade, even if both have the same exchange current densities (green curve). We therefore set out to develop a catalyst with such a Tafel slope. We reasoned that Ni would be more basic, and hence shift the pre-equilibrium from $1e^-$ (which gives a 60 mV Tafel) to $2e^-$ (which gives a 30 mV Tafel slope).

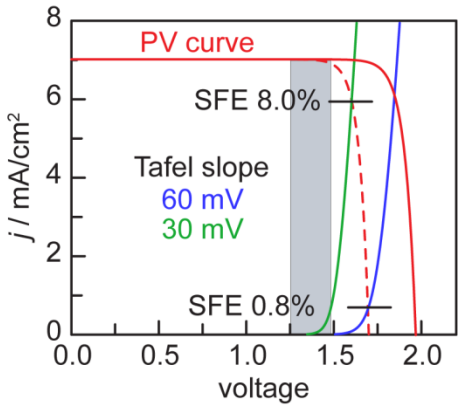

Figure 12. *i*-V curve of PV overlaid with Tafel curves of 30 and 60 mV per decade. The gray bar shows the voltage range near the thermo-dynamic potential of water splitting.

---

[16] "High-efficiency photoelectrochemical hydrogen production using multijunction amorphous silicon photoelectrodes." Rocheleau, R. E.; Miller, E. L.; Misra, A. *Energy Fuels* **1998**, *12*, 3.

[17] "Design and characterization of a robust photoelectrochemical device to generate hydrogen using solar water splitting." Kelly, N. A.; Gibson, T. L. *Int. J. Hyd. Energy* **2006**, *31*, 1658.

[18] "A monolithic photovoltaic-photoelectrochemical device for hydrogen production via water splitting." Khaselev, O.; Turner, J. A. *Science* **1998**, *280*, 425.

[19] "One-step method to produce hydrogen by a triple stack amorphous-silicon solar-cell." Lin, G. H.; Kapur, M.; Kainthla, R. C.; Bockris, J. O'M. *Appl. Phys. Lett.* **1989**, *55*, 386.

[20] "Photoelectrochemical production of hydrogen: engineering loss analysis." Rocheleau, R. E.; Miller, E. L. *Int. J. Hydrogen Energy* **1997**, *22*, 771.

Our efforts to prepare Ni-based OECs were rewarded with the discovery of a NiB_i catalyst. Cyclic voltammograms (CVs) of borate-buffered Ni^{2+}, pH 9.2 electrolytes displayed features consistent with the growth of a surface adsorbed species, along with a sharp catalytic wave. Sustained electrolysis of such Ni^{2+} electrolytes at fixed potential results in the progressive increase in current density over time, as a dark brown film becomes visible on transparent electrode substrates and grows in thickness. Films with sub-nanometer to micron thickness are readily accessible, by simply varying the deposition time.

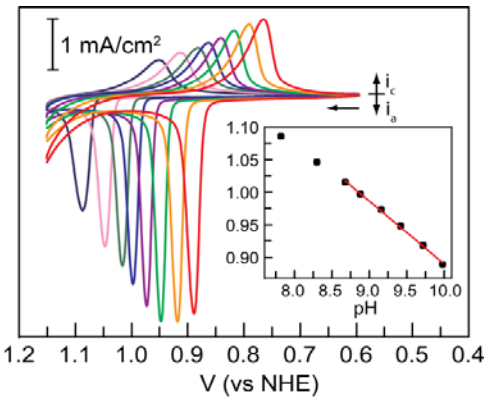

Figure 13. CVs (50mV/s) of a NiB_i catalyst film at pH values of 7.8, 8.3, 8.7, 8.9, 9.2, 9.4, 9.7, and 10.0 (from left to right). The inset shows a linear fit of the peak potential with pH, with a slope of –96 mV per pH unit.

The pH dependence of the redox waves (Figure 13) of NiB_i films indicate a $2e^-$, $3H^+$ PCET transformation between oxidized and reduced states, as has been proposed for the dimerization of Ir(IV) hydro-hydroxo species to form iridium oxide.[21,22] As such, of fundamental interest to us is the electron transfer kinetics of the Ni^{2+} to Ni^{3+} transformation that engenders film deposition, and also leads to this complex coupled multi-electron, multi-proton transition in deposited films. We find that ultrathin NiB_i films (<10 nm), for which internal electron transfer barriers are negligible, do indeed display Tafel slopes of 30 mV/decade. Future studies will be undertaken on molecular Ni compounds to shed light the proton-electron transfer dynamics of film deposition and O_2 evolution.

[21] "A voltammetric investigation of the charge storage reactions of hydrous iridium oxide layers." Burke, L. D.; Whelan, D. P. *J. Electroanal. Chem.* **1984**, *162*, 121.

[22] "A new interpretation of the charge storage and electrical conductivity behaviour of hydrous iridium oxide." Burke, L. D.; Whelan, D. P. *J. Electroanal. Chem.* **1981**, *124*, 333.

3. Cumulative Personnel

Faculty

Daniel G. Nocera

Postdoctoral Students

Ronny Costi
Mircea Dincă
Matthew Kanan
Joep J. H. Pjipers
Elizabeth Young

Graduate Students

Casandra Cox
Michael Huynh
Andrew Ullman
Yogi Surendranath

4. Collaborations

David Britt (Department of Chemistry at UC Davis): in situ EPR studies of active catalyst.

Vladimir Bulović (Department of Electrical Engineering at MIT): Co metal thin films for interface between soft semiconductors and catalyst, for the construction of the artificial leaf

Tonio Buonasissi (Department of Electrical Engineering at MIT): Construction of the artificial leaf based on Si.

Vittal K. Yachandra and Junko Yano (Lawrence Berkeley National Labs): in situ X-ray absorption studies on catalysts thin films

Arthur Esswein (Sun Catalytix): High activity thin film catalysts

Steven Reece (Sun Catalytix): Construction of triple junction Si artificial leaf.

5. Publications

Thesis

1. "Oxygen Evolution Mediated by Co-based Thin Film Electrocatalysts"; Yogesh Surendranath, Ph.D. Thesis, Massachusetts Institute of Technology, 2011.

Manuscripts

1. "Cobalt–Phosphate Oxygen–Evolving Compound"; Matthew Kanan, Yogesh Surendranath, and Daniel G. Nocera, *Chem. Soc. Rev.* **2009**, *38*, 109–14.
2. "Chemistry of Personalized Solar Energy"; Daniel G. Nocera, *Inorg. Chem.* **2009**, *48*, 10001–7.
3. "A Nickel–Borate Oxygen Evolving Catalyst that Functions under Benign Conditions"; Mircea Dincă, Yogesh Surendranath and Daniel G. Nocera, *Proc. Natl. Acad. Sci. U.S.A.* **2010**, *107*, 10337–41.
4. "EPR Evidence for Co(IV) Species Produced During Water Oxidation at Neutral pH"; J. Gregory McAlpin, Yogesh Surendranath, Mircea Dincă, Troy A. Stitch, Sebastian Stoian, William H. Casey, Daniel G. Nocera and R. David Britt, *J. Am. Chem. Soc.* **2010**, *132*, 6882–3.
5. "Structure and Valency of a Cobalt–Phosphate Water Oxidation Catalyst Determined by in Situ X–ray Spectroscopy"; Matthew W. Kanan, Junko Yano, Yogesh Surendranath, Mircea Dincă, Vittal K. Yachandra and Daniel G. Nocera, *J. Am. Chem. Soc.* **2010**, *132*, 13692–701.
6. "Direct Formation of a Water Oxidation Catalyst from Cobalt Thin–Films"; Elizabeth R. Young, Daniel G. Nocera and Vladimir Bulović, *Energy Environ. Sci.* **2010**, *3*, 1726–8.
7. "Mechanistic Studies of the Oxygen Evolution Reaction by a Cobalt–Phosphate Catalyst at Neutral pH"; Yogesh Surendranath, Matthew W. Kanan, Daniel G. Nocera, *J. Am. Chem. Soc.* **2010**, *132*, 16501–9.
8. "Solar Energy Supply and Storage for the Legacy and Nonlegacy World"; Timothy R. Cook, Dilek K. Dogutan, Steven Y. Reece, Yogesh Surendranath, Thomas S. Teets and Daniel G. Nocera, *Chem. Rev.* **2010**, *110,* 6474–502.
9. "Highly Active Cobalt Phosphate and Borate Based Oxygen Evolving Anodes Operating in Neutral and Natural Waters"; Arthur S. Esswein, Yogesh Surendranath, Steven Y. Reece and Daniel G. Nocera, *Energy Environ. Sci.* **2011**, *4*, 499–504.
10. "Bidirectional and Unidirectional PCET in a Molecular Model of a Cobalt–Based Oxygen Evolving Catalyst"; Mark D. Symes, Yogesh Surendranath, Daniel A. Lutterman and Daniel G. Nocera, *J. Am. Chem. Soc.* **2011**, *133*, 5174–7.
11. "Oxygen Evolution Reaction Chemistry of Oxide–Based Electrodes"; Yogesh Surendranath and Daniel G. Nocera, *Prog. Inorg. Chem.* **2011**, *57*, 505–60.

12. “Photo–Assisted Water Oxidation with Cobalt–Based Catalyst formed from Thin–film Cobalt Metal on Silicon Photoanodes”: Elizabeth R. Young, Ronny Costi, Daniel G. Nocera and Vladimir Bulović, *Energy Environ. Sci.* **2011**, *4*, 2058–61.

13. “Electronic Structure Description of a $[Co(III)_3Co(IV)O_4]$ Cluster: A Model for the Paramagnetic Intermediate in Cobalt–Catalyzed Water Oxidation”; J. Gregory McAlpin, Troy A. Stich, C. André Ohlin, Yogesh Surendranath, Daniel G. Nocera, William H. Casey and R. David Britt, *J. Am. Chem. Soc.* **2011**, *133*, 15444–15452.

14. “Light–induced Water Oxidation at Silicon Electrodes Functionalized with a Cobalt Oxygen Evolving Catalyst”; Joep J. H. Pijpers, Mark T. Winkler, Yogesh Surendranath, Tonio Buonassisi and Daniel G. Nocera, *Proc. Natl. Acad. Sci. U.S.A.* **2011**, *108*, 10056–61.

15. “Wireless Solar Water Splitting using Silicon–Based Semiconductors and Earth Abundant Catalysts”; Steven Y. Reece, Jonathan A. Hamel, Kimberly Sung, Thomas D. Jarvi, Arthur J. Esswein, Joep J. H. Pijpers and Daniel G. Nocera, *Science*, **2011**, *334*, 645–8.

16. “Artificial Leaf”; Daniel G. Nocera, *Acc. Chem. Res.* **2012**, *45*, 767**–**76.

17. “Interplay of Oxygen Evolution Kinetics and Photovoltaic Power Curves on the Construction of Artificial Leaves”; Yogesh Surendranath, D. Kwabena Bediako and Daniel G. Nocera, *Proc. Natl. Acad. Sci. U.S.A.* **2012**, *109*, 15617–21.

Patents

1. “Catalyst materials, electrodes, for photosynthetic replications and other electrochemical techniques”; Daniel G. Nocera, Matthew W. Kanan, Yogesh Surendranath, Mircea Dincă, Daniel A. Lutterman, Steven Y. Reece and Arthur J. Esswein; MIT Case No. 13101; U.S. Patent Appl. No. 12/486,694; 17 June 2009.

2. “Catalytic materials, photoanodes and photoelectrochemical cells for water electrolysis and other electrochemical techniques”; Daniel G. Nocera, Matthew W. Kanan, Yogesh Surendranath, Steven Y. Reece and Arthur J. Esswein; MIT Case No. 13393; U.S. Patent Appl. No. 12/643,872; 21 December 2009.

3. “Catalytic materials, photoanodes and photoelectrochemical cells for water electrolysis and other electrochemical techniques”; Daniel G. Nocera, Thomas A. Moore, Matthew W. Kanan, Yogesh Surendranath, , Steven Y. Reece and Arthur J. Esswein; MIT Case No. 13394; U.S. Prov. Pat. Appl. No. 12/643,704; 21 December 2009.

4. “Cobalt–based Water Oxidation Catalyst on Thin Film Cobalt Anodes”; Valdimir Bulovic, Elizabeth R. Young and Daniel G. Nocera, U.S. Prov. Pat. Appl. No. 61/375,729; 20 August 2010.

5. “Methods for Forming Electrodes for Water Electrolysis and Other Electrochemical Techniques”; USTPO Appl. No. 13213690, 24 August 2011.

6. Transitions

Science in the AFOSR has been transitioned to the technology sector. Water splitting catalysts and the artificial leaf are covered under a broad, sweeping patent, which is licensed to Sun Catalytix. Work has led to 9 inventions disclosures, 45 filed patents, and 2 issued licenses of the technology. Non-provisional patent filings have been made for both of these cases, which are now in the examination phase in the U.S. and other target countries.

Sun Catalytix is a renewable fuels and energy storage startup company based in Cambridge, MA. The company was founded by the PI and spun-out of MIT. Sun Catalytix is applying the founding intellectual property as well as new innovations from its world-class team of chemists and engineers to the development of renewable, clean, and cost-effective energy technologies. The company is backed by the Tata Group, Polaris Venture Partners. Sun Catalytix has 30 full-time employees.

7. Interactions

1. Truman Lecture; Sandia National Laboratories; Albuquerque, NM; 8 January 2009.
2. Sharp Technologies; Chiba, Japan; 14 January 2009.
3. Honda; Tokyo, Japan; 14 January 2009.
4. MIT Japan Club; Tokyo, Japan; 14 January 2009.
5. 11th Annual ILP Conference in Japan; Tokyo, Japan; 16 January 2009.
6. Davos World Economic Forum, Energy; Davos, Switzerland; 29 January 2009.
7. Davos World Economic Forum, Nanoscience; Davos, Switzerland; 29 January 2009.
8. NSF CCI Symposium; Ventura, CA; 31 January 2009.
9. GRC on Solar Fuels; Ventura, CA; 4 February 2009.
10. Colloquium Series on Energy; University of Pennsylvania; Philadelphia, PA; 7 February 2009.
11. Woodward Lecture, Harvard University, Cambridge, MA; 9 February 2009.
12. AIP Annual Meeting; Harvard Club; New York City, NY; 11 February 2009.
13. Polaris Ventures; Waltham, MA; 12 February 2009.
14. AAAS Annual Meeting; Chicago, IL; 13 February 2009.
15. Institute of Chemical Sciences and Engineering; University of Lausanne; Lausanne, Switzerland; 18 February 2009.

16. United States Senate, Energy Briefing; Washington, DC; 24 February 2009.
17. United States Congress, Energy Briefing; Washington, DC; 24 February 2009.
18. Emerson Lecture; Emory University; Atlanta, GA; 2 March 2009.
19. Johnston Lecture; Emory University; Atlanta, GA; 3 March 2009.
20. Polaris Ventures Portfolio Meeting; Boston, MA; 4 March 2009.
21. F.O.R.E.S.T. Symposium; Harvard University; Cambridge, MA; 5 March 2009.
22. GRC Inorganic Mechanisms; Galveston, TX; 9 March 2009.
23. Materials Research Laboratory; California Institute of Technology; Pasadena, CA; 18 March 2009.
24. ACS Inorganic Awards Address; 237th ACS National Meeting; Salt Lake City, UT; 23 March 2009.
25. Aspen Environmental Forum; Aspen, CO; 26 March 2009.
26. Department of Chemistry; Michigan State University; East Lansing, MI; 31 March 2009.
27. ARCH–Polaris, telecom; 1 April 2009.
28. Bourke Symposium; Aspen, CO; 4 April 2009.
29. Birch Lecture; Australian National University; Canberra, Australia; 15 April 2009.
30. Birch Lecture; Australian National University; Canberra, Australia; 16 April 2009.
31. Department of Chemistry; University of Maine; Orono, ME; 22 April 2009.
32. Sigma Xi Distinguished Lecture; University of Maine; Orono, ME; 22 April 2009.
33. Annual Undergraduate Lecture; California Institute of Technology; Pasadena, CA; 1 May 2009.
34. Modern Optical Seminar (Harrison Howe Labs); MIT; Cambridge, MA; 5 May 2009.
35. Plenary Lecture, ACHEMA 2009; Frankfurt, Germany; 13 May 2009.
36. Plenary Lecture ACS CERMACS, Cleveland, OH; 21 May 2009.
37. DOE Photosynthesis Efficiency Workshop; Albuquerque, NM; 23 May 2009.
38. Award Lecture, Intergovernmental Organization on Renewable Energy; United Nations, New York, NY; 11 June 2009.
39. Plenary Speaker; NAGC Workshop; Cypress Greece; 17 June 2009.
40. Eni S.p.A.; Milan Italy; 22 June 2009.
41. ACS NORM 2009; Tacoma, WA; 29 June 2009.
42. Plenary Speaker; Symposium on Recent Development of Luminescent Metal Complexes as Emerging Functional Materials"; Tokyo Institute of Technology; Tokyo, Japan, 3 July 2009.

43. 18th ISPPCC; Sapporo, Japan; 5 July 2009.
44. United States Senate, Energy Storage Briefing; Washington, DC; 16 July 2009.
45. Plenary Speaker, First Chemical Sciences and Society Symposium; Kloster Seeon, Germany; 23–25 July 2009.
46. Berry Lecture; Telluride Science Research Center; Telluride, CO; 4 August 2009.
47. Argonne National Laboratory; Argonne, IL; 7 August 2009.
48. Symposium on The Physical Chemistry of Photon to Fuel Conversion; 238th ACS National Meeting; Washington, D.C.; 16 August 2009.
49. August–Wilhelm–von–Hofmann–Lecture, German Chemical Society; Frankfurt, Germany; 30 August 2009.
50. Symposium on Chemistry for a Sustainable World, CUSO; Villars, Switzerland; 31 August 2009.
51. Symposium on Chemistry for a Sustainable World, CUSO; Villars, Switzerland; 1 September 2009.
52. Symposium on Chemistry for a Sustainable World, CUSO; Villars, Switzerland; 2 September 2009.
53. BES Council on Chemical and Biochemical Sciences, U.S. DOE; Washington, DC; 10 September 2009.
54. Enertech 2009; Boston, MA; 10 September 2009.
55. Knight Fellows Lecture; MIT; Cambridge, MA; 15 September 2009.
56. Northeastern University (Department of Chemistry); Boston, MA; 16 September 2009.
57. X Prize Lecture; MIT, Cambridge, MA; 23 September 2009.
58. EmTech 2009; Technology Review; Cambridge, MA; 24 September 2009.
59. Chesonis Portfolio Lecture; Cambridge, MA; 25 September 2009.
60. North American Forum; Ottawa, Canada; 6 October 2009.
61. CTO Forum; Chevron Corporation; San Ramon, CA; 9 October 2009.
62. Solar to Fuels Symposium; Energy Futures Lab, Imperial College; London, England; 12 October 2009.
63. ARPA–E Solar to Fuels Workshop; Arlington, VA; 21 October 2009.
64. PopTech, Camden, ME; 23 October 2009.
65. Plenary Lecture, Molecular Science for Solar Fuels; Sigtuna, Sweden, 1 November 2009.
66. Mitsui Corporation; Cambridge, MA; 5 November 2009.

67. Pauling Medal Symposium; Portland, OR; 7 November 2009.
68. University of Southern California, Energy Lab; Los Angeles, CA; 10 November 2009.
69. TOTAL; Cambridge, MA; 12 November 2009.
70. ACS Inorganic Awards Lecture; Northwestern University (Department of Chemistry); Evanston, IL; 13 November 2009.
71. ILP Research and Development Conference; Cambridge, MA; 17 November 2009.
72. Harvard University; Cambridge, MA; 24 November 2009.
73. Symposium on Chemistry and Physics of Carbon Dioxide: Challenges and Applications, CEA, Saclay France; 14 December 2009
74. Lavoisier Lecture; Paris, France; 15 December 2009.
75. Lavoisier Lecture; Paris, France; 16 December 2009.
76. Lavoisier Lecture; Paris, France; 17 December 2009.
77. Sigma Xi Lecture, Naval Research Laboratory; Alexandria, VA; 7 January 2010.
78. Eastman Chemical; Kingston, TN; 11 January 2010.
79. Eastman Chemical; Kingston, TN; 12 January 2010.
80. Perspectives on Energy and Climate; Kuwait Foundation for the Advancement of Science; Kuwait; 18 January 2010.
81. Kuwait Institute for Scientific Research; Kuwait; 19 January 2010.
82. Gordon Research Conference, Protein Cofactors and Radicals; Ventura, CA; 24 January 2010.
83. The Artificial Leaf, Lorentz Center, University of Leiden; Leiden, Netherlands; 2 February 2010.
84. ISEEE Distinguished Lectureship, The Institute for Sustainable Energy, Environment and Economy (ISEEE), University of Calgary; Calgary, Canada; 11 February 2010.
85. UCLA, California NanoSystems Institute, Los Angeles, CA; 16 February 2010.
86. Public Lecture, William D. Smart Lecture; University of West Florida; Pensacola, FL; 18 February 2010.
87. William D. Smart Lecture; University of West Florida; Pensacola, FL; 19 February 2010.
88. Billing–Croft Lecture; Whiting School of Engineering, Johns Hopkins University; Baltimore, MD; 23 February 2010.
89. Capitol Hill, U.S. Senate, Briefing, 1 March 2010.
90. ARPA–E Summit, Washington D.C.; 2 March 2010.
91. MITEI Press Conference, MIT; Cambridge, MA, 6 March 2010.

92. Robert W. Murray Lecture; University of Missouri at St. Louis; St. Louis, MO; 8 March 2010.
93. Marcus Lecture; Washington University; 9 March 2010.
94. ACS Lecture, Cincinnati–Dayton ACS Section; Cincinnati, OH; 10 March 2010.
95. World Affairs Council; San Francisco, CA; 12 March 2010.
96. Edmonton Distinguished Lecture; University of Alberta; Edmonton, Canada; 15 March 2010.
97. Kings College, Department of Chemistry; Edmonton, Canada; 15 March 2010.
98. CIC Distinguished Lecture; University of Alberta; Edmonton, Canada; 15 March 2010.
99. ACS Eminent Scientist Lecture, 239th American Chemical Society Meeting; San Francisco, CA; 22 March 2010.
100. Union League of Philadelphia; MITOR (Delaware Section); Philadelphia, PA; 5 April 2010.
101. Franklin & Marshall College; Lancaster, PA; 6 April 2010.
102. CRC Lecture, ExxonMobil; Galveston, TX; 15 April 2010.
103. Director's Lectureship, Los Alamos National Laboratory; Los Alamos, NM; 20 April 2010.
104. Derby Lecture, University of Louisville; Louisville, KY; 3 May 2010.
105. Derby Lecture, University of Louisville; Louisville, KY; 4 May 2010.
106. MSU Commencement Adders, Michigan State University; East Lansing, MI; 7 May 2010.
107. Durham Lectures, University of Durham, Durham, England; 10 May 2010.
108. Durham Lectures, University of Durham, Durham, England; 12 May 2010.
109. Durham Lectures, University of Durham, Durham, England; 13 May 2010.
110. Edward Teller Lecture, University of California at Davis, Davis, CA; 17 May 2010.
111. Phillips Academy, Andover, MA; 19 May 2010.
112. University of California at Irvine (Department of Chemistry); Irvine, CA; 21 May 2010.
113. Public Lecture, Cambridge, MA; 23 May 2010.
114. 2010 Molecular Frontiers Symposium; The Royal Swedish Academy of Sciences; Stockholm, Sweden; 3–5 June 2010.
115. Symposium Complex Materials for Energy Applications, Center for Nanomaterials Design and Assembly, Michigan State University, East Lansing, MA; 15 June 2010.

116. Gordon Research Conference, Inorganic Chemistry; University of New England; Biddeford, ME; 20 June 2010.
117. Eni S.p.A., Novara, Italy; 29 June 2010.
118. Solar Frontiers Center, MIT–Eni Workshop; Milan, Italy; 30 June 2010.
119. Royal Society Discussion, Sustainable Planet: Challenges for Science, Technology and the Structure of Society, Kavli Royal Society Centre; Milton Keynes, England; 12–14 July 2010.
120. XXIII IUPAC on Photochemistry; Ferarra, Italy; 16 June 2010.
121. Ciamician–Paternò Symposium, Photosciences a Look into the Future; Ferarra, Italy; 17 June 2010.
122. C1 Chemistry for Resource and Energy Management; University of Hamburg; Hamburg Germany; 19 June 2010.
123. C1 Chemistry for Resource and Energy Management; University of Hamburg; Hamburg Germany; 19 June 2010.
124. C1 Chemistry for Resource and Energy Management; University of Hamburg; Hamburg Germany; 19 June 2010.
125. Challenges in Inorganic and Materials Chemistry (ISACS3); Hong Kong, China; 23 July 2010.
126. Plenary Lecture, ICCC39; Adelaide, Australia; 28 July 2010.
127. AFOSR Bioenergy Program; Arlington, VA; 30 July 2010.
128. 3rd International IUPAC Conference on Green Chemistry; Ottawa, Canada; 17 August 2010.
129. Symposium on AES Science and Technology; 240th ACS National Meeting; Boston, MA; 23 August 2010.
130. Symposium on Ligand Design and Metal Behavior; 240th ACS National Meeting; Boston, MA; 25 August 2010.
131. Symposium on Molecular Systems for Efficient Solar Energy Conversion and Storage; 240th ACS National Meeting; Boston, MA; 26 August 2010.
132. Symposium on Mastery of Technology Convergence and Disruptive Technologies: New Organizational and Investment Models; Scottsdale, AZ; 29 September 2010.
133. Roseman Lecture; Johns Hopkins University (Department of Chemistry); Baltimore, MD; 7 October 2010.
134. SMArchS Colloquium; MIT (Department of Architecture) Cambridge, MA; 8 October 2010.
135. United Oil Products; Chicago, IL; 12 October 2010.

136. MITOR, Cape Cod, MA; 14 October 2010.
137. 26th Annual International Conference on Soils, Sediments, Water, and Energy; University of Massachusetts; Amherst, MA; 19 October 2010.
138. First Year Program Lecture Series, Texas A&M University; College Station, TX; 26 October 2010.
139. Clearfield Lecture (Department of Chemistry); Texas A&M University; College Station, TX; 26 October 2010.
140. GE Solar Fuels Symposium; General Electric, Global Research Center; Schenectady, NY; 2 November 2010.
141. University of Delaware (Department of Chemistry); Newark, DE; 4 November 2010.
142. TOTAL; Cambridge, MA; 9 November 2010.
143. Walton Lecture, Purdue University (Department of Chemistry); West Lafayette, IN; 11 November 2010.
144. Plenary Lecture, 6th Asian Photochemistry Conference; Wellington, New Zealand; 15 November 2010.
145. MacDiarmid Institute; Wellington, New Zealand; 18 November 2010.
146. Knight Lecture, MIT (School of Arts, Humanities and Social Sciences); Cambridge, MA; 23 November 2010.
147. Zing Solar Fuels / Photochemistry Conference 2010; Puerto Morelos Mexico; 2 December 2010.
148. B. J. Nelson Lecture; Harvey Mudd College (Office of the President); 10 December 2010.
149. Symposium on Molecular Photonics; ACS Pacifichem, Honolulu, HI; 15 December 2010.
150. Symposium on Light Driven Generation of Hydrogen from Water; ACS Pacifichem, Honolulu, HI; 16 December 2010.
151. Symposium on The Construction of Photofunctional Supramolecular Metal Complexes; ACS Pacifichem, Honolulu, HI; 19 December 2010.
152. Klemm Lecture, University of Oregon (Department of Chemistry); Eugene, OR; 14 January 2011.
153. Chemical Heritage Foundation, Philadelphia, PA; 1 February 2011.
154. Reilly Lecture; University of Notre Dame; (Department of Chemistry); South Bend, IN; 7 February 2011.
155. Reilly Lecture; University of Notre Dame; (Department of Chemistry); South Bend, IN; 8 February 2011.

156. Reilly Lecture; University of Notre Dame; (Department of Chemistry); South Bend, IN; 9 February 2011.
157. Materials in Catalysis; Berlin, Germany; 21 February 2011.
158. MIT Energy Conference; Boston, MA; 5 March 2011.
159. Harvard Club of Washington; Potomac School, Washington DC; 11 March 2011.
160. Michael Faraday Lecture, Jawaharlal Nehru Centre for Advanced Scientific Research, Bangalore, India; 21 March 2011.
161. EmTech India Conference; Bangalore, India; 22 March 2011.
162. Reliance; Mumbai India; 24 March 2011.
163. Charles Lathrop Parsons Award Symposium; 241st ACS National Meeting; Anaheim, California; 27 March 2011.
164. ACS Award in Organometallic Chemistry Symposium; 241st ACS National Meeting; Anaheim, California; 27 March 2011.
165. Nobel Laureate Signature Award for Graduate Education in Chemistry Symposium; 241st ACS National Meeting; Anaheim, California; 28 March 2011.
166. Frick Chemistry Laboratory Dedication Symposium; Princeton University; Princeton, NJ; 9 April 2011.
167. Plenary Lecture, Porphyrins and Porphyrias 2011; Cardiff, Wales, United Kingdom; 13 April 2011.
168. 2nd Annual Brooklyn Frontiers in Science Public Lecture; Brooklyn, NY; 14 April 2011.
169. Kapp Lecture, Virginia Commonwealth University; 21 April 2011.
170. Northeast Section of the ACS; Cape Cod Energy Cafe; Hyannis, MA; 29 April 2011.
171. National Academy of Sciences; Washington, DC; 1 May 2011.
172. Ohio State University; Institute for Materials Research; Columbus, OH; 3 May 2011.
173. Clean Energy Ventures; MIT; Cambridge, MA; 4 May 2011.
174. Eisenberg Symposium; University of Rochester; Rochester, NY; 20 May 2011.
175. Aspen Environmental Forum; Aspen, CO; 2 June 2011.
176. The Seminar; Miami, FL; 5 May 2011.
177. 33rd DOE Solar Photochemistry Meeting; Wintergreen, VA; 7 June 2011.
178. 2011 Air Force Office of Scientific Research (AFOSR) Bioenergy Meeting; Arlington, VA; 8 June 2011.
179. Crossroads Conference; MIT; Cambridge, MA; 16 June 2011.
180. 5th Gerischer Symposium; Berlin, Germany; 23 June 2011.

181. Eni–MITEI Symposium; Milan, Italy; 29 June 2011.
182. Eni–MITEI Symposium; Milan, Italy; 30 June 2011.
183. ISACS4 Workshop; Royal Society of Chemistry; Cambridge, MA; 5 July 2011.
184. European Symposium on Organic Chemistry; Crete, Greece; 10 July 2011.
185. University of Athens; Athens, Greece; 18 July 2011.
186. Chemistry of Solar Energy Symposium; IUPAC World Chemistry Congress; Puerto Rico; 2 August 2011.
187. Innovation Symposium; IUPAC World Chemistry Congress; Puerto Rico; 2 August 2011.
188. UNESCO Energy Conference; Towards Global Artificial Photosynthesis, Energy, Nanochemistry & Governance; Lord Howe Island, Australia; 15 August 2011.
189. NSF Catalytic Chemistry Workshop; Denver, Colorado; 27 August 2011.
190. Symposium on Computational Modeling of Photo–catalysis and Photo–induced Charge Transfer Dynamics on Surfaces; 242nd National ACS Meeting; Denver, Colorado; 28 August 2011.
191. Symposium on Fifty Years of Inorganic Chemistry: A Celebration of Past, Present, and Future; 242nd National ACS Meeting; Denver, Colorado; 29 August 2011.
192. Symposium on Fifty Years of Inorganic Chemistry: A Celebration of Past, Present, and Future; 242nd National ACS Meeting; Denver, Colorado; 30 August 2011.
193. Symposium on Towards Earth Abundant Solar Photocatalysis; 242nd National ACS Meeting; Denver, Colorado; 31 August 2011.
194. BSA Distinguished Lectureship; Brookhaven National Laboratory; Upton, NY; 8 September 2011.
195. Innovation Day; Chemical Heritage Foundation; Philadelphia, PA; 20 September 2011.
196. ACS Connecticut Valley Section 100th Anniversary Symposium; Hartford, CT; 1 October 2011.
197. 3rd Erlangen Symposium on Redox–Active Metal Complexes: Control of Reactivity via Molecular Architecture; Erlangen, Germany; 5 October 2011.
198. PCET 2011 'From Biology to Catalysis', Richelieu, France; 11 October 2011.
199. Science Bio–Inspirée et Applications, la Fondation Écologie d'Avenir, Paris, France ; 14 October 2011.
200. A.R. Gordon Distinguished Lectureship; University of Toronto; Toronto, Canada; 18 October 2011.

201. A.R. Gordon Distinguished Lectureship; University of Toronto; Toronto, Canada; 19 October 2011.
202. A.R. Gordon Distinguished Lectureship; University of Toronto; Toronto, Canada; 20 October 2011.
203. John K. and Delores Stille Science Symposium; Colorado State University; Fort Collins, CO; 22 October 2011.
204. Renewable Energy for Our Future; Bilkent University; Ankara, Turkey; 26 October 2011.
205. BM Holding; Ankara, Turkey; 26 October 2011.
206. Knight Fellows; MIT; Cambridge, MA; 3 November 2011.
207. Vale Innovation Sustainability Program; MIT Sloan School of Management; Cambridge, MA; 7 November 2011
208. SBE'S Conference on Electrofuels Research; DOE ARPA–E; Providence, RI; 7 November 2011.
209. Total–MIT Program; MIT; Cambridge, MA; 8 November 2011.
210. Solar Fuels; NREL–University of Colorado; Boulder, CO; 10 November 2011.
211. Purves Lectureship; McGill University; Montreal, Canada; 15 November 2011.
212. 2011 MRS Fall Meeting; Materials Research Society; Boston, MA; 29 November 2011.
213. Zing Coordination Chemistry Conference 2011; Xcaret, Mexico; 10 December 2011.
214. Synergy between Experiment and Computation in Energy – Looking to 2030 (ENCON1); SEAS, Harvard University; Cambridge, MA; 12 January 2012.
215. 14th National Symposium in Chemistry; Chemical Research Society of India; Trivandrum, India; 3 February 2012.
216. Sixteenth Mesilla Chemistry Workshop on Ligand–Based Control of Spin and Reactivity in Metal Complexes; Mesilla, New Mexico; 12 February 2012.
217. International Workshop on Advanced Materials – IWAM 2012; Ras Al Khaimah Center for Advanced Materials (RAK–CAM); United Arab Emirates; 19 February 2012.
218. Güraller ArtCraft; Istanbul, Turkey; 27 February 2012.
219. Earth-Abundant Materials for Critical Technologies; American Physical Society March Meeting 2012; Boston, MA; 29 February 2012.
220. ACSA100; Association of Collegiate Schools of Architecture; Boston, MA; 2 March 2012.
221. SmartSurfaces2012: Solar & Biosensor Applications; Dublin, Ireland; 6 March 2012.

222. Lewis Lecture; University of Cambridge; Cambridge, England; 13 March 2012.
223. Lewis Lecture; University of Cambridge; Cambridge, England; 14 March 2012.
224. MIT Energy Conference: Insight and Innovation in Uncertain Times; Cambridge, MA; 16 March 2012.
225. ACS Award in Pure Chemistry Symposium; 243rd ACS National Meeting; San Diego, CA; 25 March 2012.
226. A Career in Actinide Science: Tribute to Lester Morss; 243rd ACS National Meeting; San Diego, CA; 27 March 2012.
227. Solar Energy Conversion and Utilization for Fuels and Energy Production Symposium; 243rd ACS National Meeting; San Diego, CA; 27 March 2012.
228. ACS Award in Inorganic Chemistry Symposium; 243rd ACS National Meeting; San Diego, CA; 28 March 2012.
229. Fifth Annual ANSWER Symposium, Solar Fuels; Northwestern University; Evanston, IL; 25 April 2012.
230. Clean Energy Ventures; Sloan School, MIT; Cambridge, MA; 2 May 2012.
231. Naval Seas System Command, United States Navy; 16 May 2012.
232. Jean Dreyfus Boissevain Lecture; University of Massachusetts Dartmouth; Dartmouth, MA; 14 May 2012.
233. Jean Dreyfus Boissevain Lecture; University of Massachusetts Dartmouth; Dartmouth, MA; 15 May 2012.
234. Jean Dreyfus Boissevain Lecture; University of Massachusetts Dartmouth; Dartmouth, MA; 15 May 2012.
235. Honeywell Leadership Conference; Phoenix, AZ; 22 May 2012.
236. Remsen Award Lecture; MARM 2012; University of Maryland Baltimore County; Baltimore, Maryland; 31 May 2012.
237. 2nd International Symposium on Natural and Artificial Photosynthesis, Bioenergetics and Sustainability, Nanyang Technological University; Singapore; 11 June 2012.
238. 75th Jubilee Distinguished Lecture, Hong Kong Polytechnic University, Hong Kong, China; 13 June 2012.
239. Hong Kong University, Department of Chemistry; Hong Kong, China; 14 June 2012.
240. Huang Rayson Lecture, Hong Kong University, Hong Kong, China; 15 June 2012.
241. Hong Kong University, Department of Chemistry; Hong Kong, China; 18 June 2012.
242. Eni-MIT Symposium, Milan, IT; 27 June 2012.
243. ACA Wood Award Lecture; Boston, MA; 1 August 2012.

244. GRS Lecture; Electron Donor Acceptor GRC; Salve Regina University; Newport, RI; 4 August 2012.
245. 2012 Air Force Office of Scientific Research (AFOSR) Bioenergy Meeting; Arlington, VA; 10 August 2011.
246. ACS Nanoscience Symposium; ACS Philadelphia; Philadelphia, PA: 21 August 2012.
247. Think Green2; Harvard University; Cambridge, MA; 18 September 2012.
248. Musselman Lecturer; Gettysburg College; Gettysburg, PA; 20 September 2012.
249. Musselman Lecturer; Gettysburg College; Gettysburg, PA; 20 September 2012.
250. Musselman Lecturer; Gettysburg College; Gettysburg, PA; 21 September 2012.
251. Musselman Lecturer; Gettysburg College; Gettysburg, PA; 21 September 2012.
252. Penn State University; Department of Chemistry; State College, PA; 27 September 2012.
253. Harvard College Fund Symposium; Harvard College; Cambridge, MA: 29 September 2012.
254. Gerhard Ertl Center Inauguration; Technical University of Berlin; Berlin, Germany; 8 October 2012.
255. Knight Fellows; MIT; Cambridge, MA; 11 October 2012.
256. Welch Conference; Houston, TX; 22 October 2012.
257. CNO Lecturer; Naval War College; Newport RI; 1 November 2012
258. Indiana University; Department of Chemistry; Bloomington, IN; 7 November 2012.
259. Jefferson Lecturer; University of Virginia; Charlottesville, VA; 16 November 2012.
260. Bayer Lecture; University of Pittsburgh, Pittsburgh, PA; 28 November 2012.
261. Bayer Lecture; University of Pittsburgh, Pittsburgh, PA; 29 November 2012.
262. AICHE; Billerica, MA; 6 December 2012.
263. Monte Jade New England Science and Technology Association (MJNE); Microsoft Center; Cambridge, MA; 8 December 2012.
264. Southern Methodist University; Department of Chemistry; Houston, TX; 11 December 2012.
265. Energy and Climate Symposium; Knight Journalism School; MIT; Cambridge, MA; 19 December 2012.

8. Honors

Awards

1. Honorary Fellow, Indian Academy of Sciences, 2012
2. ACS Remsen Award, 2012

3. Time Magazine, Innovation of the Year, 2011
4. Honorary Fellow, Chemical Research Society of India, 2011
5. Elizabeth Wood Award, American Crystallographic Association, 2010
6. MJ Collins Award, CEM Corporation, 2010
7. Roseman Award, Johns Hopkins University, 2010
8. Honorary Degree, Michigan State University, 2010
9. Elected to the National Academy of Sciences, 2009
10. Time Magazine 100 Award, 2009
11. United Nations IREO Science and Technology Award, 2009
12. ACS Award in Inorganic Chemistry, 2009

Honorary Lectureships

1. Bayer Lecturer, University of Pittsburgh, 2012
2. Jefferson Lecture, University of Virginia, 2012
3. Musselman Lecture, Gettysburg College, 2012
4. Rayson Huang Lecture, University of Hong Kong, 2012
5. 75th Jubilee Distinguished Lecture, Hong Kong Polytechnic University, 2012
6. Jean Dreyfus Boissevain Lecture, University of Massachusetts Dartmouth, 2012
7. Lewis Lectures; University of Cambridge, 2012
8. Purves Lectureship; McGill University, 2011
9. John K. and Delores Stille Science Lectureship, Colorado State University, 2011
10. A.R. Gordon Distinguished Lectureship, University of Toronto, 2011
11. BSA Distinguished Lectureship, Brookhaven National Laboratory, 2011
12. Kapp Lecture, Virginia Commonwealth University, 2011
13. Michael Faraday Lecture, Jawaharlal Nehru Centre, 2011
14. Reilly Lectures, Notre Dame, 2011
15. Klemm Lecture, University of Oregon, 2011
16. B. J. Nelson Lecture, Harvey Mudd College, 2010
17. Walton Lecture, Purdue University, 2010
18. Clearfield Lecture, Texas A&M, 2010
19. Roseman Symposium, Johns Hopkins University, 2010
20. Durham Lectures, Durham University, 2010
21. Teller Lecture, University of California at Davis, 2010

22. Derby Lecture, University of Louisville, 2010
23. Director's Lecture, Los Alamos National Laboratory, 2010
24. CRC Lecture, ExxonMobil, 2010
25. CIC Edmonton Distinguished Lecture, 2010
26. ACS Eminent Scientist Lectureship, 2010
27. Leopold Marcus Lecture, Washington University, 2010
28. Robert W. Murray Lecture, University of Missouri at St. Louis, 2010
29. Billing–Croft Lecture, Johns Hopkins University, 2010
30. William D. Smart Lecturer, University of West Florida, 2010
31. ISEEE Distinguished Lectureship, University of Calgary, 2010
32. Sigma Xi Distinguished Lecture, Naval Research Laboratory, 2010
33. Lavoisier Lectures, University of Paris, 2009
34. August Wilhelm von Hofmann Lecture, German Chemical Society, 2009
35. Berry Lecture, Telluride Science Research Center, 2009
36. Sigma Xi Distinguished Lecture, University of Maine, 2009
37. Birch Lecture, The Australian National University, 2009
38. Johnston Lecture, Emory University, 2009
39. Emerson Lecture, Emory University, 2009
40. R.B. Woodward Lecture, Harvard University, 2009
41. Truman Distinguished Lecture, Sandia National Laboratory, 2009